

See discussions, stats, and author profiles for this publication at: <https://www.researchgate.net/publication/350185973>

# Laser micromanufacturing of electrospray thruster emitters from sheets of polytetrafluoroethylene SPACE PROPULSION 2020+1

Conference Paper · March 2021

CITATIONS

0

READS

192

3 authors:



**Sahil Maharaj**

The University of Manchester

2 PUBLICATIONS 0 CITATIONS

[SEE PROFILE](#)



**Katharine Lucy Smith**

The University of Manchester

91 PUBLICATIONS 853 CITATIONS

[SEE PROFILE](#)



**Olivier J Allegre**

The University of Manchester

41 PUBLICATIONS 350 CITATIONS

[SEE PROFILE](#)

Some of the authors of this publication are also working on these related projects:



Development of advanced techniques for aerodynamic assessment of blunt bodies in hypersonic flow [View project](#)



Ultrafast Laser-Materials Micro-Structuring with Phase Only Spatial Light Modulators [View project](#)

# Laser micro-manufacturing of electro spray thruster emitters from sheets of polytetrafluoroethylene

SPACE PROPULSION 2020+1

17 – 18 – 19 MARCH 2021

S Maharaj<sup>(1)</sup>, O Allegre<sup>(1)</sup> and KL Smith<sup>(1)</sup>

(1) University of Manchester, Oxford Rd, Manchester, M13 9PL, UK, Email: sahil.maharaj@manchester.ac.uk

**KEYWORDS:** propulsion, electro spray, manufacturing, plate emitter, laser

## ABSTRACT:

Electro spray thrusters are a type of micro propulsion system that have the potential to expand the scope of missions available to small satellites. In order to maximise the thrust, electro spray thrusters are typically comprised of an array of emitters. As such, one of the major challenges that needs to be addressed is manufacturing working emitters small enough that the array can still be used on a small satellite. Traditionally, these emitters are capillaries, which are manufactured through techniques such as photolithography and deep reactive ion etching [1–3]. While accurate, these methods require a substantial time and cost investment. By using a hole shaped emitter, rather than a capillary shaped emitter, these emitters can instead be manufactured through the use of laser drilling, a process which has the potential to be up to six times faster than traditional methods.

This paper aims to investigate the feasibility of using this manufacturing technique to construct an emitter by drilling holes in a flat plate. By examining the suitability of a variety of different materials, this paper seeks to find the ideal manner in which an electro spray thruster can be manufactured using laser drilling. This is done by examining the effectiveness of each material when used in an emitter, by using computer modelling to determine the strength of the electric field generated around each material. The effect of various parameters, such as thickness and hole taper, on the strength of this field is also examined.

Through the use of computational modelling and analysis, it was found that PTFE, flexible PVC, PEEK and Kapton would generate the strongest electric fields. However, it was also noted that PVC would be less suitable than the other materials listed when it came to manufacturing an emitter for use in a vacuum. Additionally, it was noted that both the taper of the hole, as well as the degree of wetting influence the performance of the emitter. It was finally concluded that the rate at which the material is ab-

lated by a laser needs to be known, before the ideal material for use in an emitter can be selected.

## 1. Introduction

Electro spray (ES) propulsion is a form of electrostatic propulsion, in which a stream of charged particles are emitted from an electrolytic liquid. This is achieved by generating an electric field between the liquid and an electrode. This field focuses the liquid into a conical shape, which emits a stream of charged particles from the liquid, generating a thrust [4]. Due to the low levels of thrust generated, as well as the small size of an ES emitter, electro spray is a good candidate for use as a source of propulsion for small satellites.

The simplest ES emitter layout, referred to as a capillary emitter or a needle emitter, has the propellant fed into a capillary emitter, with an extractor electrode located a set distance away from the tip. The propellant is stored in a reservoir, and is fed into the emitter by either a pressure differential or a pump system. A potential difference is applied across the emitter and the extractor, which leads to the aforementioned electric field.

While this can be thought of as the standard ES emitter layout, other emitter types are possible. One of these is the Hole Emitter (HE), also referred to as the flat plate emitter. Here, instead of a capillary, the emitter is a flat plate with a hole (or holes) drilled through it.

Traditionally ES emitters are manufactured using techniques such as photolithography and deep reactive ion etching [1–3]. While suitable for manufacturing emitters, these methods suffer from significant drawbacks, such as a substantial time investment, and the need for highly specialised manufacturing equipment. This paper investigates the suitability of hole emitters that have been manufactured through laser drilling, which has the potential to mitigate these issues. This is done by examining the suitability of HE's made using flat plates of a variety of different materials and thicknesses. A computational physics model is employed, which determines the effect that different HE configurations have on

the strength of the generated electric field. The effect of material properties such as relative permittivity and conductivity are examined, across a range of thicknesses, in order to determine the ideal geometry. Additionally, the shape of the hole, and the degree of wetting are also examined.

In further research, these results will be considered alongside the suitability of the material for laser drilling. This includes factors such as the time it takes to be drilled, as well as the shape of the resultant hole. This will result in a trade off, where the ease of manufacture will need to be weighed up against the performance of the finished product. Once the ideal material has been selected, the emitter will be constructed and tested. It will then be compared to a capillary emitter running under similar conditions. However, this can be considered as future work which falls outside the scope of this paper, which will focus primarily on computational work.

The HE's manufactured in this investigation will consist of flat plates with an area of 5 cm by 5 cm, with a range of thicknesses. The extractor electrode is modelled as an aluminium ring electrode with a diameter of 5 mm, which is located 2 mm above the flat plate and centred on the hole. For the purposes of the study detailed in this paper a single hole is drilled in the centre, although future work will examine the effect of multiple holes.

In an investigation by Lozano, Martínez-Sánchez and Lopez-Urdiales [5], it was found that the primary factor that determines the suitability of a hole emitter is the material from which the emitter is manufactured. Specifically it was found that dielectric materials with a suitably low relative permittivity were ideal for enhancing the electric field. In a capillary emitter the capillary directs the electric field towards the tip of the emitter, resulting in a stronger electric field at the tip. Fig. 1 shows a visualisation of this effect, with the field lines "bunching up" at the tip of

This is a cross section of the flat plate ES emitter, with the dotted line being a plane of symmetry. In this diagram, the blue rectangles are the extractor electrode, the yellow rectangles is the flat plate, the cyan shape is the propellant, and the dark green rectangle is the emitter electrode. Here,  $d$  is the distance between the plate and the extractor,  $D$  is the diameter of the hole,  $t$  is the thickness of the plate, and  $D_w$  is the diameter of the extractor hole. The Taylor cone itself is modelled as a cone with a half angle ( $\beta$ ) of  $49.3^\circ$ , topped with a circle with a radius of  $r_t$ .

For the purposes of this investigation, the values of  $D$  and  $D_w$  were set to 0.2 mm and 5 mm respec-

<sup>1</sup>A right angled triangle can be drawn between the tip of the Taylor cone and the edge of the emitter, so the Pythagorean Theorem can be used.

the capillary, but being equally distributed over the hole emitter. Low permittivity materials compensate for this by allowing the electric field to be shaped by the propellant column, rather than the flat plate. A plate made of a theoretical ideal material would be modelled as a column of propellant, suspended in a vacuum. It was also noted that the material should have a low electrical conductivity ( $\sigma$ ), as an electrically conductive material would require a significantly higher voltage to generate an electric field strong enough for electrospray to occur.

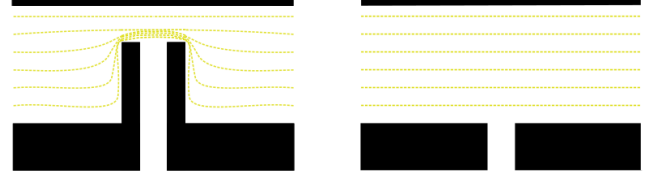


Figure 1: Difference in electric field distribution between different emitter geometries

Lozano et al. [5] experimentally examined emitters made of Polytetrafluoroethylene (PTFE); Polyethylene (PE); Polycarbonate (PC) and Polyvinyl chloride (PVC). Of these, PTFE was found to have the best performance, which corresponded to it having the lowest relative permittivity. However, in order to examine the aforementioned trade off, the specifics of each material will be examined. In order to determine the suitability of a material for electrospray, a flat plate emitter will be modelled, and the magnitude of the electrostatic field at the tip of the Taylor cone will be measured.

## 2. EMITTER GEOMETRY

In order to model the system, a simplified version of the geometry must be examined. Fig. 2 shows a depiction of the geometry of the ES system that was modelled.

tively. The value of  $d$  would determine the onset voltage for electrospray [2], and so it was set to 2 mm, meaning that the distance between the tip of the Taylor cone to the edge of the emitter was  $3.2 \text{ mm}^1$ . The value of  $r_t$  was calculated using Eq.1 [6].

$$r_t = \frac{\epsilon_o Q^{1/3}}{K} \quad \text{Eq.1}$$

Here,  $Q$  is the liquid flow rate,  $K$  is the conductivity of the propellant, and  $\epsilon_o$  is the permittivity of free space.

The electric field would be modelled for a variety of values of  $t$ . It is hoped that this would give the mini-

imum required thickness of the plate for ES to occur. While a lower value of  $t$  would reduce manufacturing complexity, it also results in a hole with a lower aspect ratio. Due to the phenomena mentioned in section 1, this would, result in a weaker electric field at the tip of the cone where ES forms, for a given applied voltage.

### 3. FEA MODEL

The model of the ES system was generated in COMSOL multiphysics, which is an FEA solver and multiphysics simulation tool. Due to the symmetric nature of the setup, only half of the rig needs to be modelled. With this in mind, the actual geometry modelled in COMSOL can be seen in Fig. 3.

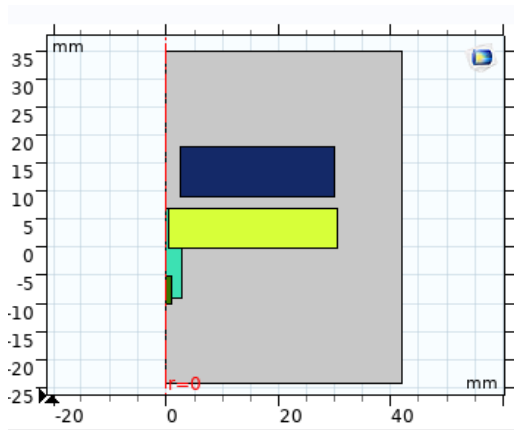


Figure 3: Geometry of flat plate emitter in COMSOL

While care was taken to ensure that the geometry would match the actual emitter layout, some concessions were made. In reality, an IDEX nanoport assembly [7] will be attached to the other side, which will feed the propellant towards the hole. This assembly will connect to both the propellant reservoir, as well as the emitter electrode. However, in both Fig.s 2 and 3, the NanoPort assembly was omitted.

Testing indicated that the inclusion of this assembly did not affect the results, and so it was not included for the sake of simplicity.

A positive voltage of 6.5 kV was generated across the emitter electrode, while the extractor electrode was set to ground. These values were chosen based on the maximum output of a FUG HCP 14-6500 high voltage power supply system [8], which is what will be used in future experimental testing. By modelling the maximum possible potential difference, the maximum possible electric field strength can be observed for each material. This can then be compared to the electric field strength required for ES emission, in order to determine if the emitter will be suitable. In reality, a lower voltage will be used whenever possible, with the reasoning behind this being explained in section 6 of this paper.

The materials examined were similar to those previously listed, with some changes. As the range of possible  $\sigma$  values for PVC is significantly large (compared to other materials) [9], two samples of PVC were examined, one which would be quite rigid (PVC-R) and one which would be flexible (PVC-F). Additionally, Polyether Ether Ketone (PEEK) and Kapton were chosen as additional materials that would be examined. PEEK has a history of successfully being used to make components for ES emitters [2, 10, 11], and its low out-gassing values make it ideal for use in a vacuum. Similarly, Kapton is traditionally used as an insulating material in vacuum products. The full list of materials chosen, as well as their relevant properties, can be seen in Tab. 1.

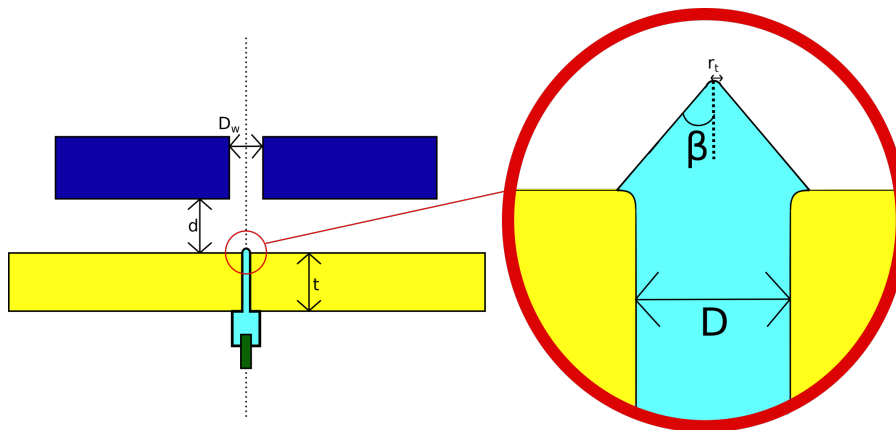


Figure 2: Visualisation of modelled geometry. Note that this is not to scale

Material	Relative permittivity	Conductivity ( $\text{S m}^{-1}$ )
PTFE	2.1	$1.00 \times 10^{-23}$
PET	2.25	$1.13 \times 10^{-13}$
PC	2.9	$1.00 \times 10^{-14}$
PVC-R	4	$1.00 \times 10^{-16}$
PVC-F	4	$1.00 \times 10^{-12}$
PEEK	3.3	$2.04 \times 10^{-15}$
Kapton	3.6	$1 \times 10^{-15}$

Table 1: Materials used in COMSOL model

Each of these properties were assigned to the flat plate in turn. For each test, the extractor and emitter electrodes were modelled as being made of aluminium, and the domain was modelled as being filled with air. The propellant was modelled as a solution of Triethylene Glycol (TEG) with dissolved Sodium Iodide (NaI). This solution had a relative permittivity of 23.69 and a conductivity of  $0.04 \text{ S m}^{-1}$ . These properties were chosen as this would be the propellant that will be used during initial experimental testing in atmosphere. During vacuum testing an ionic liquid will be used, however changing the modelled propellant to an ionic liquid resulted in a negligible change in results<sup>2</sup>. As such this propellant will be suitable for use when modelling ES in both air and vacuum.

Once the geometry and materials were modelled, the electric field was simulated. This was done for all the materials listed in Tab. 1, and for a range of thicknesses from 1 mm to 1 mm.

#### 4. COMPUTATIONAL RESULTS

Simulating the electric potential across the figure as described resulted in a potential distribution as seen in Fig. 4. Here the distribution of the potential difference across a 7mm sheet of PTFE is depicted.

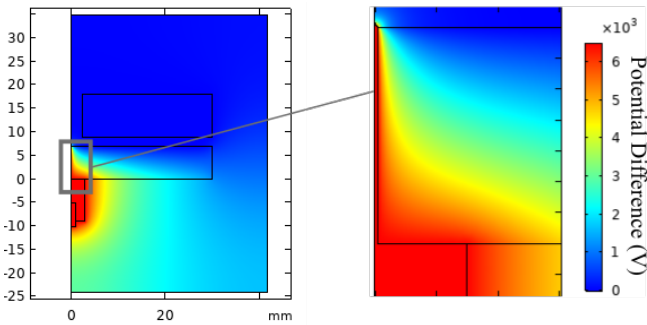


Figure 4: Potential difference distribution across rig. This shows both the entire modelled domain (left), as well as a zoomed in view of the propellant in the hole (right).

Each of the other materials and thicknesses resulted in similar figures, albeit with minor differences. Referring to Fig. 4, it can be seen that the field is

<sup>2</sup>This is due to the fact that the liquid's permittivity and conductivity have a negligible effect on the performance of the system. The conductivity of the propellant would have to drop to below  $1 \times 10^{-9} \text{ S m}^{-1}$  before a notable change in the peak electric field strength can be observed

shaped by the column of propellant, rather than the plate itself. This indicates that the electric field should be focused on the tip of the Taylor cone, which is ideal for ES.

This is proven by examining the electric field across the entire rig, which shows that the magnitude is greatest at the tip of the Taylor cone. Measuring this peak electric field strength for all cases provides the data seen in Fig. 5.

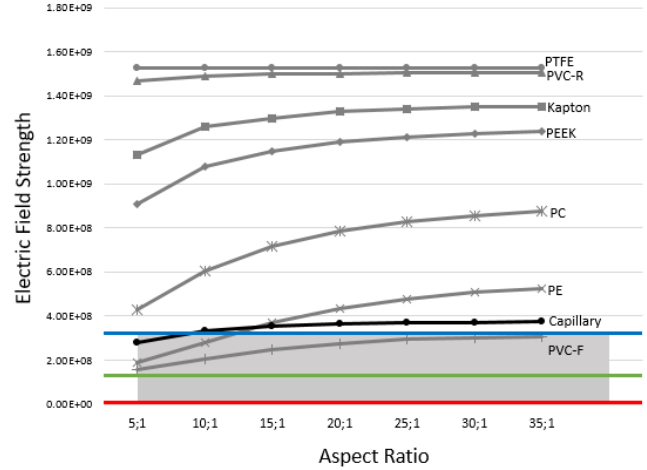


Figure 5: Peak electric field strength for all materials and thicknesses. The shaded area between the coloured lines indicates minimal required field strength.

For the purposes of comparison, these results have been compared to a traditional capillary emitter, seen in black. This emitter consisted of a stainless steel capillary, with a similar aspect ratio (AR) to the other case studies. All other parameters were the same as previously described. As a result of this comparison, the hole emitters are grouped by the aspect ratio of the holes, rather than due to the thickness of the plates. For example, a hole with a diameter of 0.2 mm through a sheet with a thickness of 7 mm would have an aspect ratio of 35:1. Examining this figure shows that for most cases increasing the aspect ratio increases the peak electric field strength, as expected. However, the field strength for rigid PVC and Teflon plateau despite the increases in AR. As these are the materials with the highest electric strength values, these might imply a maximum field strength value that can not be exceeded.

The horizontal lines were intended to show the minimum electric field lines required for ES to occur. These were calculated using three different methods. The red line was obtained using Eq.2, where  $\gamma$  is the surface tension of the propellant. This equation was adapted from Smith [12].

$$E_o = \left( \frac{4\gamma \cos(\beta)}{\epsilon_o D} \right)^{1/2} \quad \text{Eq.2}$$

The blue line was obtained using Eq.3, which was based on an equation described by Mair [13].

$$E_o = \left( \frac{4\gamma}{\epsilon_o r_t} \right)^{1/2} \quad \text{Eq.3}$$

Finally, the green line was obtained by modelling a capillary emitter at the onset of ES emission and measuring the magnitude of the peak electric field. An emitter with an aspect ratio of 35:1 was modelled, with all other geometric values the same as those previously described. The potential difference across the emitters would need to be set to the onset Voltage for electrospray. An equation for this, from Krpoun [2], can be seen in Eq.4, where  $V_o$  is the onset voltage.

$$V_o = \sqrt{\frac{0.5\gamma D}{\epsilon_o} \ln\left(\frac{0.5D+2d+2\sqrt{d(d+0.5D)}}{0.5D}\right)} \quad \text{Eq.4}$$

As the distance from the emitter to the extractor is significantly larger than the diameter of the extractor, this equation can be simplified to Eq.5.

$$V_o = \sqrt{\frac{0.5\gamma D}{\epsilon_o}} \ln \frac{4d}{r_o} \quad \text{Eq.5}$$

By depicting these three values on the graph in Fig 5, we are able to obtain a range of values for the minimum electric field strength<sup>3</sup>. This allows us to compare the performance of each material to this minimum baseline, as well as to each other. However, it should be noted that these values are all for the ideal scenario, and so the effect of other parameters such as taper and wetting must be examined.

## 5. EFFECTS OF TAPER AND WETTING

In the previously described model, there was no taper in the hole, and minimal wetting across the surface. In reality, as the aim of this project is to manufacture the rig using lasers, some taper is a possibility. This will result in the diameter of the hole closer to the extractor being of a different size to the hole further away from the emitter, similar to the depiction seen in Fig 6. For the purposes of this report, taper will be measured by the parameter  $t_p$ , which is the difference between the radii of the two holes.

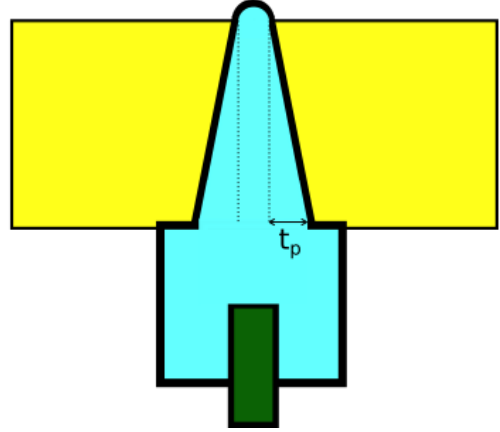


Figure 6: Visualisation of hole taper

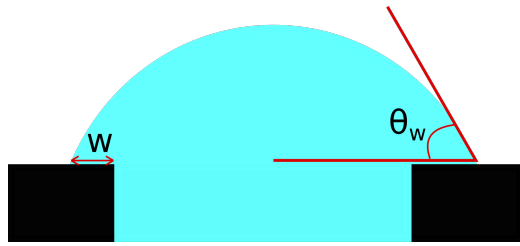
In an investigation into laser drilling of small holes, Li et al. [14] examined a range of taper angles caused by laser drilling. In holes less than 1 mm, a taper angle of 5° was found to be the maximum value. In a plate with a thickness of 7 mm a taper angle of 5° would correspond to a  $t_p$  value of 0.61 mm. With this in mind, a range of  $t_p$  values will be examined, from 0.2 mm to 1 mm.

Additionally, while the model was simulated with minimal wetting, in reality this may not be the case. Depending on the interaction between the propellant and the emitter material, the propellant may spread out over the surface of the emitter. This would likely have a negative effect on the performance, with Lozano et al. [5] describing hydrophobia being a positive attribute of a plate emitter. The degree of wetting is determined by the interfacial tension forces between [15]:

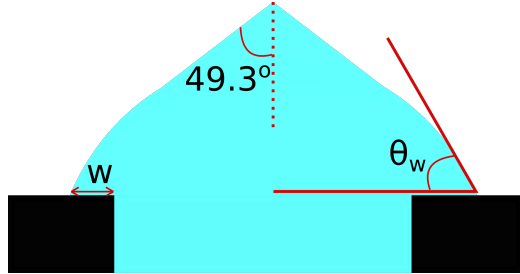
- The flat plate and the propellant
- The flat plate and the atmosphere
- The propellant and the atmosphere (the surface tension)

These factors determine the wetting angle ( $\theta_w$ ), which in turn determines the shape of the droplet. Referring to the Fig. 7a, the wetting angle of a droplet can be seen.

<sup>3</sup>It should be evident that there is a large amount of variation between these three values. As such, values will only be described as being suitable if they are significantly higher than the value calculated using Eq.3. This is elaborated upon in the discussion section



(a) Droplet wetted across surface



(b) Taylor cone formed from wetted droplet

Figure 7: Visualisation of  $w$  and  $\theta_w$

Once the electrostatic force has been applied to the droplet, the Taylor cone will then form on top of it, as seen in Fig. 7b. This is how it will be modelled in the computational model. For the purposes of simplicity, the model utilises the parameter  $w$ , which is the distance between the tip of the hole and the edge of the droplet. This proved to be easier to vary across the model than the value of  $\theta_w$ . For an ideal scenario with no wetting,  $\theta_w$  will be  $90^\circ$ , and  $w$  will be zero, which translates to a perfect Taylor cone. As  $\theta_w$  decreases,  $w$  increases, which leads to the Taylor cone having more of an irregular shape.

Similar to  $t_p$ , a range of values of  $w$  will be explored. In this case, a range of values of from 0.01 mm and 0.1 mm. These values were influenced by Reed [16], who examined how ES propellants wet across a variety of surfaces, including PTFE. They logged a range of  $\theta_w$  values from  $35^\circ$  to  $77^\circ$ , which corresponds to  $w$  values of 0.09 mm and 0.015 mm respectively. As such a range of 0.01 mm to 0.1 mm is examined.<sup>4</sup>

The simulation was run two more times, once with  $t_p$  varied, and once with  $w$  varied. In both cases, increasing the respective parameter decreased the value of the electric field strength. However, the magnitude of this change varied significantly. For  $w$ , a 7 mm thick piece of PTFE experienced a drop from  $1.53 \times 10^9 \text{ V m}^{-1}$  to  $1.15 \times 10^9 \text{ V m}^{-1}$ . This was almost a 25% decrease. A similar decrease was seen with all other materials, which can be seen in Fig. 8<sup>5</sup>.

<sup>4</sup>The relationship between  $\theta_w$  and  $w$  was calculated by assuming that the droplet would have the same cross sectional area as a hemisphere with no wetting.

<sup>5</sup>Note that for Polyethylene and flexible PVC increasing the wetting angle increases the magnitude of the electric field. This is not what was expected, but it might be because that these materials originally had quite low values for the electric field strength. As such, increasing the width of the Taylor cone might improve the field shaping effect in some manner.

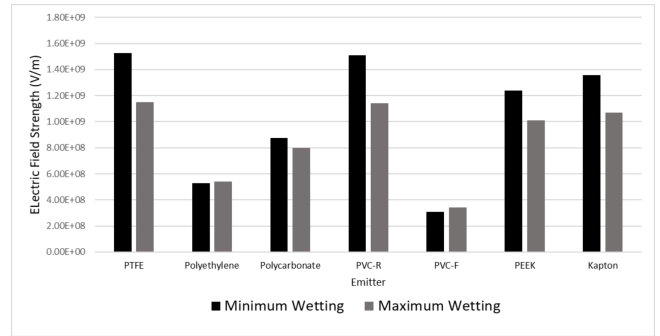


Figure 8: Effect of wetting on electric field strength

Conversely, the taper angle had a less notable effect for the range of values examined. Referring to Fig. 9, the electric field strengths at the maximum and minimum tapers can be seen. Here, the effect is much smaller, especially on the emitters which have stronger electric field strengths.

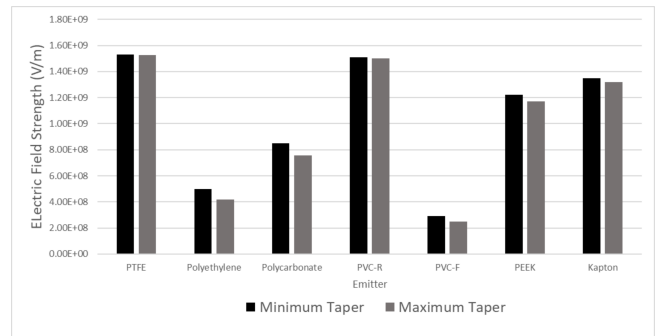


Figure 9: Effect of taper on electric field strength

## 6. DISCUSSION

Referring to Fig. 5, it can be seen that not only are many of the peak electric field strength values higher than the minimum values, they are also significantly higher than the values for a capillary emitter. This would imply that these emitters should be able to produce ES emission at voltages lower than those required for a traditional ES emitter.

It is apparent that the three values for minimum electric field strength are significantly spread out. This is due them being obtained from three different methodologies, thus making it difficult to determine the most appropriate metric for measuring the suitability of these emitters. For the purposes of comparison, Mair [13] can be treated as a worst case scenario, although all three methodologies have their limitations that need to be considered. Looking at the calculated values, the equation from Mair [13] produces a significantly higher result than the others. This is possibly due to them examin-

ing thrusters that used liquid metals as a propellant. These would have a significantly higher conductivity than the TEG/NaI mixture examined in this paper. Additionally, they assumed that the  $r_t$  value would be the same as the radius of the emitter, which was a needle with a tapered tip. As such, this value would likely be significantly higher than the actual value, which would further skew the applicability of these results.

The value from the model that was simulated for an emitter running at  $V_o$  also has some uncertainty associated with it. Note that neither Eq.3 nor Eq.2 take into account the length/AR of the emitter. Referring back to Fig. 5, it can be seen that the electric field strength for a capillary does vary as the AR decreases. So while the value presented is correct for an emitter with an AR of 35:1, if the same equation was used for an emitter with an AR of 5:1, a slightly lower value would be produced.

Finally, it should be noted that the value obtained from the equation found in Smith [12] is significantly smaller than any measured electric field. This disparity would also imply some manner of inaccuracy, as it was experimentally tested that ES does not occur at low voltages.

With this in mind, comparing the values of a given emitter to that of the capillary emitter is a better metric for measuring suitability. Experimental testing of a capillary with a AR of 10:1 resulting in ES being observed as the potential difference exceeded 2 kV. As such any value that exceeds the peak electric field strength of a capillary emitter with this value would be capable at achieving ES at a suitable potential difference.

It can be seen that PTFE has the strongest electric field strength at the tip of the Taylor cone, which is consistent with the results noted by Lozano et al. [5]. At higher AR, PVC-R has similar values to PTFE, with PEEK and Kapton also having values significantly higher than the capillary emitter. However, one important point that should be remembered is that although rigid PVC has high electric field strengths, PVC has a relatively high level outgassing [17]. As such, the lower outgassing values of PEEK and Kapton [18], as well as their history of use in vacuum, might make them more suitable for

an emitter which will be used in a vacuum.

Another benefit of PTFE, PEEK and Kapton, is that they are all inherently hydrophobic [19–21]. As an example, in the aforementioned investigation by Reed [16], Kapton had a  $\theta_w$  value of  $57^\circ$ , which corresponds to a  $w$  value of 0.185 mm. This is close to the minimum wetting described in Fig. 8, with there being less than a 3% decrease in field strength when compared to the minimum wetting scenario.

When determining the ideal thickness, some analysis is required. For PTFE, Fig. 5 shows a similar magnitude of field strength for all aspect ratios. As such, a 1 mm thick sheet would suffice. For Kapton, the final two values are of similar magnitudes, indicating that an emitter with an aspect ratio of 30:1 or higher would be necessary to maximise the field strength. For a 0.2 mm diameter hole, this would require a 6 mm sheet. Finally, PEEK does not exhibit this plateauing effect, and as such an emitter with an AR of greater than 35:1 would be required to maximise the electric field.

However, while it would be ideal to maximise the electric field strength, the necessity of this needs to be determined. As seen in Fig. 5, for PTFE, PEEK and Kapton, even the smallest AR holes still generate field strengths greater than a capillary emitter with an AR of 35:1. As such, all of these materials will be able to generate ES with an AR of 5:1, making a smaller AR suitable. Nevertheless, it is beneficial to try and maximise the field strength, since this will decrease the potential difference required for ES to occur. When testing in voltage occurs, components such as electrostatic gates and Faraday cups will need to be manufactured and purchased. Electrostatic gates can increase in price as the voltages being dealt with increase, and as such minimising the potential difference will be more economical. With this in mind, the only way an ideal AR and sheet thickness can be determined is by examining how each material reacts to laser machining. This would include examining the rate at which each material is ablated, as well as the minimum taper and diameter of holes that can be produced.

Once this is undertaken, the ideal material can be selected between PTFE, PEEK and Kapton.

## 7. REFERENCES

1. Gassend, B.L.P (2007). *A Fully Microfabricated Two-Dimensional Electro spray Array with Applications to Space Propulsion*, Doctor of Philosophy, Massachusetts Institute of Technology, Massachusetts.
2. Krpoun, R. (2009). *Micromachined Electro spray Thrusters for Spacecraft Propulsion*, Doctor of Science, École Polytechnique Federale De Lausanne, Lausanne.
3. Dandavino, S., Ataman, C., Chakraborty, S., Shea, H., Ryan, C. & Stark, J. (2013). Design and fabrication of the thruster heads for the MicroThrust MEMS electro spray propulsion system, *33rd International Electric Propulsion Conference*, pp1–8.
4. You, Z. (2017). Micropropulsion, *Micro and Nano Technologies* ed You Z (Butterworth-Heinemann) pp 295–339.
5. Lozano, P., Martínez Sánchez, M. & Lopez-Urdiales, J.M. (2004). Electro spray emission from nonwetting flat dielectric surfaces, *Journal of Colloid and Interface Sci.* **276**(2), 392–399.
6. Gamero-Castaño, M. & Fernández de la Mora, J. (2000). Direct measurement of ion evaporation kinetics from electrified liquid surfaces, *The Journal of Chemical Phys.* **113**(2) 815–832.
7. IDEX Health and Science (nd). *NanoPort Assemblies - PEEK & PTFE NanoPort Components*.
8. FuG Elektronik GmbH (2008). *High voltage power supplies HCP-series operating instructions*.
9. Titow, M.V. (1984). *PVC Technology* (Springer Science & Business Media) pp 1194-1195.
10. Lajhar, F.A.A. (2018). *Electro spray for pulmonary drug delivery*, Doctor of Philosophy, The University of Manchester, Manchester.
11. Sögaard, C., Simonsson, I. & Abbas, Z. (2019). Development and Evaluation of Polyether Ether Ketone (PEEK) Capillary for Electro spray, *ACS Omega*, **4**, 1151–1156
12. Smith, D.P.H. (1986). The Electrohydrodynamic Atomization of *Liquids IEEE Transactions on Industry Applications*, **IA-22**(3), 527–535.
13. Mair, G. (1980). Emission from liquid metal ion sources, *Nuclear Instruments and Methods*, **172**(3), 567–576.
14. Li, L., Low, D., Ghoreishi, M. & Crookall, J. (2002). Hole Taper Characterisation and Control in Laser Percussion Drilling *CIRP Annals*, **51**(1), 153–156.
15. Wayner, Jr, P.C. (1982). Interfacial profile in the contact line region and the Young-Dupre equation, *Journal of Colloid and Interface Sci.*, **88**(1).
16. Reed, G.D. (2012) *EMIIM Wetting Properties of & Their Effect on Electro spray Thruster Design*, Master of Science, California State University, Northridge.
17. Eley, R. (1975). Outgassing of vacuum materials-II *Vacuum*, **25**(11), 469-485.
18. Battes, K., Day, C. & Hauer, V. (2018). Outgassing behavior of different high-temperature resistant polymers, *Journal of Vacuum Sci. & Technology*, **36**.
19. Shyu, R.F., Yang, H., Tsai, W.R. and Tsai, J.C. (2007) Micro-ball lens array fabrication in photoresist using PTFE hydrophobic effect, *Microsystem Technologies*, **13**(11), 1601–1606.
20. Fang, Y., Hester, J.G.D., Su, W., Chow, J.H., Sitaraman, S.K. and Tentzeris, M.M. (2016). A bio-enabled maximally mild layer-by-layer Kapton surface modification approach for the fabrication of all-inkjet-printed flexible electronic devices, *Scientific Reports*, **6**(1), 39909.
21. Johansson, P., Jimbo, R., Kjellin, P., Currie, F., Chrcanovic, B.R. and Wennerberg, A. (2014). Biomechanical evaluation and surface characterization of a nano-modified surface on PEEK implants: a study in the rabbit tibia, *International Journal of Nanomedicine*, **9**, 3903.